Statistical Regression Analysis of Response of Northern Mid and Upper Tropospheric Circulation to Winter Eurasian Snow Cover Effects①

Xu Jianjun (徐建军)
Nanjing Institute of Meteorology, Nanjing 210044, China
Received January 3, 1994; revised March 21, 1994

ABSTRACT

Response for anomalous circulation in relation to snow coverage is derived by use of regression coefficients in dealing with the Eurasian snow cover time series and northern mid and upper tropospheric height data. Results show that not only does the regression response pattern represent the correlation between snow coverage and circulation change but reflects the amplitude strength in correlation cores as well, with a greater amplitude of the circulation response in the mid troposphere and remarkable equivalent barotropy in the mid to upper levels, and that the response of winter–summer circulations to winter snow cover displays noticeable stationary planetary–scale wavetrain, leading to NEUP and NPNA patterns in winter, slightly changed forms in spring months and LEU and EANA in summer time. Also, the study demonstrates that the rasponse–produced wavetrain is marked by branch and propagates energy in a wave–front manner with the energy trapped at subtropical latitudes.

Key words: Regression analysis, Tropospheric circulation, Eurasian snow cover

1. INTRODUCTION

Possible effects of snow cover on weather and climate have already drawn the attention of meteorologists. The reasons lie in that 1) a significant albedo exists over snow cover, leading to vast difference in absorbing shortwave radiation between a snow–covered area and snow–free ground; 2) snow is of poor conductivity, making for great weakening of air–ground exchange at snow regions and 3) penetration of melting snow as water into soil enhances evaporation. All these are responsible for the effects on circulation and weather of snow cover before and after its melting.

Statistical correlation studies devoted to the relationship between snow cover and weather anomaly on a local scale (*Hahn et al., 1976; Chen at al., 1979; Fu, 1980; Lu and Xu, 1992*) indicate that both are correlated to some extent and a critical factor contributing to them is the atmospheric circulation regime, which will be anomalous due to the changed transport of physical quantities caused by snow cover, thereby producing some anomaly of weather / climate. It is for this reason that the snow cover–atmospheric circulation relation has been the subject of much interest. Two approaches are adopted to this problem. One is numerical simulation, which suffers from difficulties arising due to the fact that snow cover distribution does not bear so much regularity as do external forcings like SST, thus giving rise to more or less trouble with modelling. The other is statistical correlation analysis. However, there is the rub. Correlation coefficients can reflect nothing more than the correlativities but not the

①This work is supported by the National Natural Science Foundation of Jiangsu Province, China.

degree of the resulting anomaly of different segments. A regression chart developed by Nakamura et al. (1987) as a new kind of statistical analysis is adopted in the present work. As an effective means in dealing with the influence of snow cover on circulation, this method consists of separating from the whole circulation field the response in relation to a particular time sequence of snow cover. Consequently, the snow cover–circulation relation is revealed on the basis of the derived anomalous part due to snow with the aid of the regression chart analysis.

II. DATA AND METHOD

1. *Data*

The data used come from 1976–1987 monthly mean Eurasian snow coverage (EASC) derived by a NOAA / NESS satellite and northern monthly average 100 and 500 hPa grided height for the same periods with winter, spring and summer regimes represented by the data of January, April and July, separately.

2. *Brief Outline of the Method Employed*

Following Nakamura et al., $H_t(\lambda,\varphi)$ denotes the height, S_t the measured EASC, which is then normalized for calculation, $H_s(\lambda,\varphi)$ the linear regression coefficient of the height towards the EASC (the horizontal pattern of these coefficients is referred to as the regression response pattern in relation to EASC). $H_s(\lambda,\varphi)$ is found out by means of the method of least squares error, with the square error obtained by

$$\varepsilon_s^2(\lambda,\varphi)=\sum_t[H_t(\lambda,\varphi)-\overline{H}(\lambda,\varphi)-H_s(\lambda,\varphi)(S_t-\overline{S})]^2 \ , \tag{1}$$

with $H_s(\lambda,\varphi)$ to be given by

$$H_s(\lambda,\varphi)=\frac{\sum_t(H_t(\lambda,\varphi)-\overline{H}(\lambda,\varphi))(S_t-\overline{S})}{\sum_t(S_t-\overline{S})^2} \ , \tag{2}$$

where $\overline{H}(\lambda,\varphi)$ and $\overline{S}$ stand for the time means of the height and EASC, respectively. (2) indicates that $H_s(\lambda,\varphi)$ is a quantity dependent of time t but having the height dimension, and capable of displaying, to significant extent, the amplitude vigor of the center of the response action. F–test is used in verifying regression statistics and the statistic $F_s(\lambda,\varphi)$ takes the form

$$F_s(\lambda,\varphi)=RG_s^2(\lambda,\varphi)/RE_s^2(\lambda,\varphi) \ , \tag{3}$$

where

$$RG_s^2(\lambda,\varphi)=H_s^2(\lambda,\varphi)\sum_t(S_t-\overline{S})^2 \ ,$$

$$RE_s^2(\lambda,\varphi)=(N-2)^{-1}\sum_t[H_t(\lambda,\varphi)-\overline{H}(\lambda,\varphi)-H_s(\lambda,\varphi)(S_t-\overline{S})]^2 \ ;$$

In this study $N=21$ and the specified credibility $=0.05$ so that F_s should never be smaller than 4.4.

III. ANALYSIS OF ATMOSPHERIC CIRCULATION REGRESSION RESPONSE PATTERNS

1. *Horizontal Distribution Features of Winter Response Field*

The horizontal distribution of the regression response of January mean 500 hPa height to

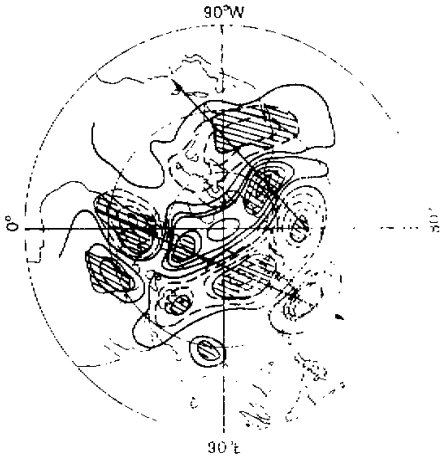

Fig. 1. January horizontal pattern of the regression coefficient $H_z(\lambda,\varphi)$ for 500 hPa height toward the EASC, contoured at 10.0. The area of $F_z \geqslant 4.4$ is shaded and passes the test at 0.05 credibility.

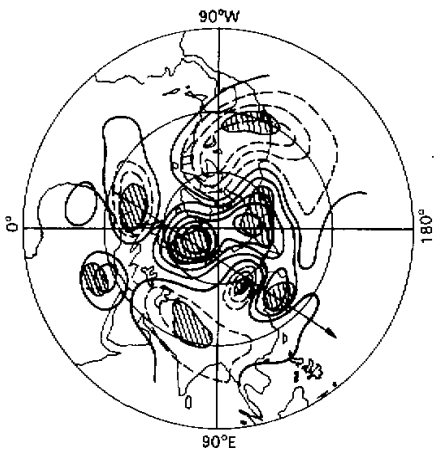

Fig. 2. Winter horizontal pattern of the regression coefficient $H_z(\lambda,\varphi)$ for 100 hPa height toward the EASC, contoured at 1.0. The area of $F_z \geqslant 4.4$ is shaded and passes the test at 0.05 credibility.

the EASC is illustrated in Fig.1. First of all we can see that the amplitude response differs from place to place, with stronger negative cores over the south of Iceland, in the Caspian Sea, Siberia, Lake Baikal, Sea of Okhotsk, south of the Aleutians and in North America, all responsible for lowered 500 hPa height at these localities and, in contrast, the positive counterparts found in Arctic, west of the Urals, to the south of the Mediterranean, Gulf of Alaska and waters of Japan, causing the rise of the height. Next, one can see the corrspondence of these cores to the longwave troughs / ridges in this season, implying that the core pattern is characteristic of stationary waves. Finally, these cores are evidently situated north of 30°N, suggesting that the EASC acts as a trapper of the steady wave pattern, making it appear poleward of subtropical latitudes only.

Viewed on a steady wavetrain basis, two patterns exist, one emanating from the coastal area in the west of Eurasia via the Urals and Lake Baikal and reaching the neighborhood of Japan, a wavetrain that is called a North Europe / Asia to Pacific (NEUP) pattern, and the other stretching from the North Pacific south of the Aleutains to Alaska and then to North America, a wavetrain termed a NPNA pattern. Under the NEUP effect, such winter stationary systems as the West Europe coastal ridge, East Europe trough, northern Qinghai–Xizang Plateau ridge and the south part of the East–Asian deep trough have their amplitudes decreased, implying the reduction (amplification) of meridional (zonal) circulation over the path, thus hindering cold air from southward invasion. And under the NPNA action the trough northwest of the east Asian deep trough, Alaska ridge and North America deep trough have their amplitudes increased, strengthening (tapering off) meridional (zonal) circulation, thereby causing cold weather in the south of the continent.

Of interest is the comparison of the NEUP and NPNA patterns to the winter stationary teleconnections EU and PNA proposed by Wallace et al (1981). The NEUP has four

oscillation cores lying to the north as compared to three for EU; the NPNA possesses only three such cores with the subtropical one out of being in contrast to PNA. The difference demonstrates that the EASC–caused anomaly is no more than part of the abnormality in atmospheric circulations as a whole, which therefore offers merely interpretations of some facts of anomalous weather, e.g., precipitation. As a result, it is groundless to attempt to procure a good correspondence of local weather anomaly to EASC change.

Further analysis demonstrates that lying to the south of the NEUP is a weaker wavetrain, both being of the same origin. Consequently, the latter can be regarded as a branch of the former. However, the distribution of their oscillation centers shows that those of the same sign are located roughly on an arc line, which leads us to believe that waves travel not simply through the oscillation cores along its track but via an arc–form wave front composed of multiple centres as well, as with a point source of light wherefrom the propagation takes the form of a wave front. This may be considered as energy dispersion due to the interaction of a few planetary wavetrains. Evidently, such dispersion occurs mainly in a particular path for a given wavetrain.

Needless to say, statistical credibility test is indispensable to the determination of the presence of NEUP, NPNA and their branches appearing as wave fronts. One can see from the shaded areas of Fig.1 that the statistic F_s around the respective cores are >4.4, suggesting their passage of test at 0.05 credibility, which serves as sound evidence demonstrating the presence of these systems with their subsystems.

Inspection of this figure indicates that 1) beyond those cores at the segments south of the Aleutains and Alaska, the amplitude centers are in rough coincidence with the oscillation ones of the 500 hPa response field except that the oscillation is far weaker. This fact illustrates that the EASC response field is of equivalent barotropy and the response amplitude gets smaller as a function of the height; 2) the upper tropospheric NEUP remains as it used to but its vigor decreases with its reinforced branch, a phenomenon indicating that the wavetrain is a deep barotropic system. It is noted that the NPNA is no longer existent in its place because of the difference in the response of the oscillation cores, suggesting that it is a shallow system with baroclinity in some localities.

2. *Horizontal Distribution Features of Spring Response Field*

Fig. 3 portrays the regression response of April 500–hPa height to January EASC. Its comparison to Fig.1 shows the changes as follows. First, where the winter Arctic vortex frequently occurs a stronger positive amplitude core now makes its appearance, thus weakening the gyre, with the intensity of the amplitude cores of the other places reduced slightly. Second, the NEUP wavetrain is maintained but with the core's position moved a little westward and the amplitude phase opposite to that observed in winter. This amplifies meridional motion over Eurasia, giving rise to cold weather of spring in the south. Moreover, a planetary–scale wavetrain running from the subtropical Pacific via Alaska, North Canada and South Greenland into the North Atlantic comes into being in lieu of the NPNA pattern with a weaker one to the south.

As shown in Fig. 4, there still exists the NEUP, exhibiting an equivalent barotropic structure while the stronger 500–hPa NPNA has disappeared, thereby intensifying the amplitude of the faint wave at lower latitudes.

Inspection of the mid–upper tropospheric spring response fields shows that the steady wave equivalent barotropical structure remains stable over the Eurasian–Pacific, and, like the winter pattern, there exists energy propagation feature as a wave front with noticeable

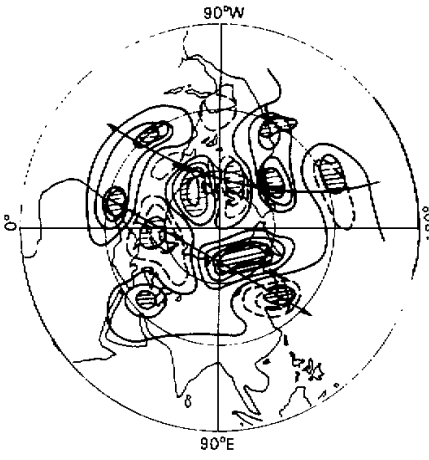

Fig. 3. The same as in Fig.1 but for spring.

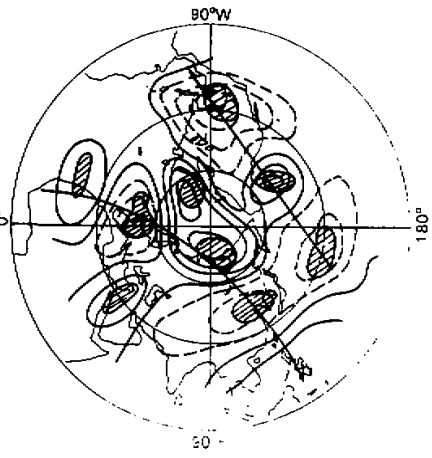

Fig. 4. Like Fig. 2 but for spring.

difference between the upper and lower levels over the Pacific–North America. Moreover, the amplitude core is moved closer to low latitudes than in the winter pattern, suggesting that the latitudes at which the spring planetary wavetrain is trapped are lower than in the winter case.

3. *Horizontal Distribution Features of Summer Response Field*

As shown in Fig. 5, there is great change in the July 500 hPa response to January EASC as compared to the January and April patterns. A semi–meridional small–scale wavetrain shows up in Europe and is termed latitudinal European (LEU) pattern; another stronger

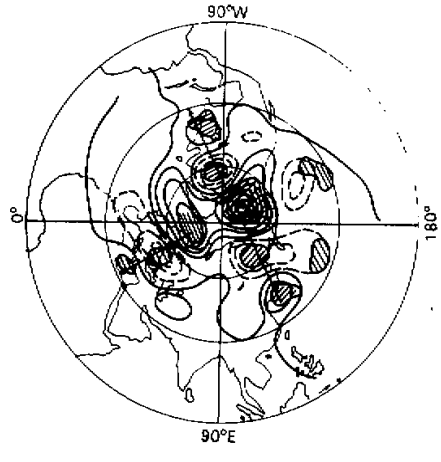

Fig. 5. As in Fig. 1 but for summer.

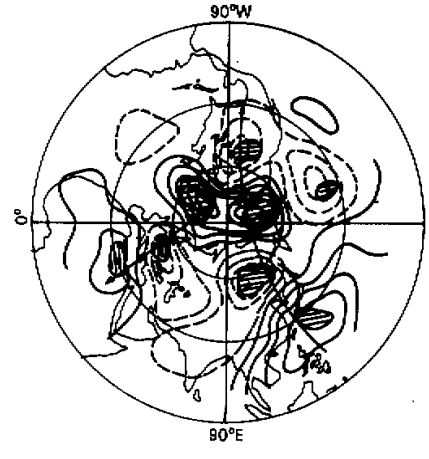

Fig. 6. As in Fig.2 except for summer and contour of 0.5.

planetary wavetrain stretches over the East Asian seaboard, Bering Strait, Canada and east North America, implying that the change in the eastern Asian deep trough can affect the analog of east North America, a wavetrain called the East Asian–North America (EANA) pattern. Beyond that, a weaker branch appears to the north of the EANA wavetrain.

In Fig. 6 both the LEU and EANA patterns are existent, situated a bit westward and marked by enlarged amplitude horizontal scale as compared to the mid tropospheric case, with the EANA's branch reinforced.

Inspection of the summer response at 100 and 500 hPa indicates that the stationary planetary wave exhibits its stable equivalent barotropy in the eastern and western hemispheres alike. Further, the remote response of summer height to winter EASC is responsible for the steady EANA wavetrain. Therefore, the EASC can affect pressure change in North America and east Asian seaboard by modifying the east Asian subtropic high.

IV. CONCLUSIONS

From the foregoing analysis we come to the following conclusions.

1. The regression coefficients of the heights toward EASC time series can be used to effectively separate the response regime of atmospheric circulation to snow cover. Not only does the response pattern reflect their correlativity but the amplitude vigor of the correlation cores as well.

2. As seen in the response to winter EASC, the 500–hPa circulation shows much stronger amplitude than the 100–hPa counterpart but their amplitude cores are roughly coincided, indicative of equivalent barotropy and these cores correspond to the troughs / ridges of winter steady wave, thus causing changes in zonal / meridional motions.

3. The response differs from season to season. The winter response produces NEUP and NPNA wavetrains, the former (latter) being deep (shallow) and found at 500 and 100 hPa (only at 500 hPa); the spring response shows that NEUP remains but with its position slightly changed and vigor decreased, and that NPNA has given its way to another; the summer response exhibits the meridional LEU and EANA wavetrains at both levels. The response–produced steady wavetrains in all the three seasons are subjected to trapping at subtropical latitudes.

4. Branch occurs in the stationary planetary wavetrains due to response to EASC and it advances as a wave front, with a certain wave track particularly remarkable.

REFERENCES

Chen Lieting et al. (1979), Effect of Qinghai–Xizang Plateau winter–spring snow cover on atmospheric circulation and rainfall over South China in the following wet season, *Symposium on Mid and Long Term Hydrological and Meteorological Prediction* (*I*), Water–Resources & Electricity Press, Beijing 185–194 (in Chinese).

Fu Zongbin (1980), Relation of change in northern winter to spring ice / snow coverage to low–temperature summer in NE China, *Acta Meteor. Sinica*, **38(2)**: 187–192 (in Chinese).

Hahn, D.G. and J. Shukla (1976), An apparent relationship between Eurasian snow cover and Indian monsoon rainfall, *J. Atmos. Sci.*, **33**: 2461–2462.

Lu Juezhong and Xu Jianjun (1992), Teleconnection between Eurasian snow cover and eastern China rainfall, in Long–Term Weather Prediction and Sun–Earth Relation Research, China Ocean Press, Beijing 62–69 (in Chinese).

Nakamura, M. et al. (1987), Horizontal structure and energetics of the Northern Hemisphere wintertime teleconnection patterns, *J. Atmos. Sci.*, **44**: 3377–3391.

Wallace, J. M. and D.S. Gutzler (1981), Teleconnection in the geopotential height field during the Northern Hemisphere winter, *Mon. Wea. Rev.*, **109**: 784–813.